# NON CONFORMING SPACE-TIME GRIDS FOR THE WAVE EQUATION : A NEW APPROACH

Laurence Halpern

**Abstract.** We present a new method to design non-conforming space-time algorithms for the wave equation. It relies on the use of the Schwarz Waveform Relaxation method, and allows strong velocity contrasts, together with the use of weakly dispersive meshes.

## §1. Introduction

When solving evolution problems in heterogeneous media, it is often desirable to use non conforming grids in space and time, such a case may be when different time scales in different media are present. When dealing with wave propagation, this issue is most crucial, due to numerical dispersion. For example, let us consider the one dimensional wave equation

$$\frac{1}{c^2(x)}\frac{\partial^2 u}{\partial t^2} - \frac{\partial^2 u}{\partial x^2} = 0.$$

In order to minimize the dispersion, the mesh sizes need to be close to the CFL condition everywhere. When using the leap-frog scheme for instance, the CFL number $\gamma = c\Delta t/\Delta x$ must be smaller than $1$. For $\gamma = 1$, the scheme is exact.
The question of designing a mesh refinement in time and space arises in two ways. The first application is when one wants to use a finer space discretisation in a small part $\Omega_1$, with a roughly constant speed. In order to keep $\gamma$ close to 1, one has to discretize time in the same fashion. The second application is when the velocity is larger in a part $\Omega_1$, if a constant space mesh is required, a finer mesh in time is needed in $\Omega_1$. We summarize and generalize with $I$ domains $\Omega_i$ such that

(I) either $c$ is constant in $\mathbb{R}$, the space meshes $\Delta x_i$ are different, $c\Delta t_i/\Delta x_i$ is a constant ,

(II) or the speed in each $\Omega_i$ is a constant $c_i$, the space mesh $\Delta x$ is a constant, the time steps $\Delta t_i$ are such that $c_i\Delta t_i/\Delta x$ is a constant.

In both cases $\gamma$ has to be constant, as large as possible, depending on the scheme.
This problem has been widely studied in particular for the transport equation, in connection with problem (I). The first paper is [1], where the Lax-Wendroff scheme is proved to be stable with interpolatory transmission conditions. In [2, 3], the leapfrog scheme is studied. Stability

problems for Dirichlet boundary data are reported. New transmission conditions using discrete energy estimates are proposed, and proved to be stable.
Our approach is totally different and addresses in particular problems (I) and (II). It relies on the use of Schwarz waveform relaxation algorithms (SWR). The wave equation in $\mathbf{R} \times (0,T)$ is first written as a collection of wave equations in $\Omega_i \times (0,T)$ with perfectly transmitting conditions on the boundaries between neighboring subdomains. The solution is calculated through a Schwarz algorithm. In the case of piecewise constant velocities, it converges in two iterations on appropriate time windows. We then discretize in time and space using finite volumes, which enables us to naturally take the transmission conditions into account. The space and time steps are chosen independently and optimally in each subdomain, and the solution is transmitted to the neighbour by a projection procedure. For the leapfrog scheme, the total procedure is stable and convergent in both cases. The tools are energy estimates in case (I) and Laplace transform in case (II). It is numerically shown to keep the second order accuracy.

## §2. About the Schwarz Waveform relaxation method

We consider the second order , one dimensional wave equation with variable wave speed,

$$\mathcal{L}(u) : \frac{1}{c^2(x)}\frac{\partial^2 u}{\partial t^2} - \frac{\partial^2 u}{\partial x^2}, = 0 \tag{1}$$

on the domain $\mathbb{R} \times (0,T)$ with initial conditions $u(\cdot,0) = p$ and $\frac{\partial u}{\partial t}(\cdot,0) = q$.

We first define the classical Schwarz waveform relaxation algorithm in the case of two subdomains. We introduce two overlapping subdomains $\Omega_1 = (-\infty, L)$ and $\Omega_2 = (0, +\infty)$. At step $k$, we solve two subproblems in $\Omega_i \times (0,T)$, with a Dirichlet data on the boundary given by the previous step in the other domain. The solution in $\Omega_i \times (0,T)$ at step $k$ is called $u_i^k$. The classical Schwarz algorithm extended to space-time domains is then given by:

$$\begin{cases} (\frac{1}{c^2}\frac{\partial^2}{\partial t^2} - \frac{\partial^2}{\partial x^2})u_i^{k+1} = 0 \text{ in } \Omega_i \times (0,T) \text{ for } i = 1,2, \\ u_i^{k+1}(.,0) = p \text{ in } \Omega_i, \ \dfrac{\partial u_i^{k+1}}{\partial t}(.,0) = q \text{ in } \Omega_i, \\ u_1^{k+1}(L,.) = u_2^k(L,.), \quad u_2^{k+1}(0,.) = u_1^k(0,.) \text{ in } (0,T). \end{cases} \tag{2}$$

**Theorem 1.** *For the Schwarz algorithm (2), convergence is achieved in a finite number of iterations,* $k \geq \dfrac{T \sup c(x)}{L}$.

*Proof.* The proof can be found in [5], and relies on the finite speed of propagation. We describe it here in the case of constant velocity. Consider the errors $U_i^k = u_i^k - u$. They satisfy system (2) with zero initial values. Using d'Alembert's formula, we have

$$\begin{aligned} &\text{for } x - ct > 0, \quad U_2^{k+1}(x,t) = 0, \\ &\text{for } x - ct < 0, \quad U_2^{k+1}(x,t) = U_1^k(0, t - \frac{x}{c}), \end{aligned} \tag{3}$$

and

$$\begin{aligned} &\text{for } x + ct < L, \quad U_1^{k+1}(x,t) = 0, \\ &\text{for } x + ct > L, \quad U_1^{k+1}(x,t) = U_2^k(L, t - \frac{L-x}{c}). \end{aligned} \tag{4}$$

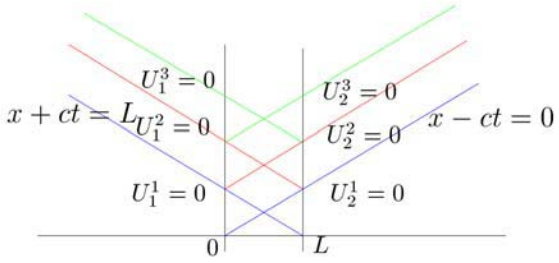


Figure 1: Evolution of the Schwarz algorithm with Dirichlet transmission conditions

We can now see the end of the proof on Figure 1 using (3) and (4) : at step $k$, $U_1^k$ vanishes for $x + ct \leq kL$ and $U_2^k$ vanishes for $x - ct \geq -(k-1)L$. Thus $U_1^k$ and $U_2^k$ vanish identically on the time interval $(0, T)$ if $T \leq kL/c$. □

This shows first that the classical method, even with two subdomains, is extremely slow, and secondly that it needs a large overlap to increase the convergence speed. Note that for any transmission conditions, the error $U_1^k$ on the left is a function of $x - ct$ only, while on the right the error $U_2^k$ is a function of $x + ct$ only. This in turn implies the following identities for $k \geq 1$ and any positive time

$$\begin{cases} \left(\dfrac{\partial}{\partial x} + \dfrac{1}{c}\dfrac{\partial}{\partial t}\right) U_2^k(L,t) = 0, \\ \left(\dfrac{\partial}{\partial x} - \dfrac{1}{c}\dfrac{\partial}{\partial t}\right) U_1^k(0,t) = 0. \end{cases}$$

This observation leads to the following simple but important

**Theorem 2.** *The transmission conditions defined by*

$$\begin{aligned} \left(\frac{\partial}{\partial x} + \frac{1}{c}\frac{\partial}{\partial t}\right) u_1^{k+1}(L,t) &= \left(\frac{\partial}{\partial x} + \frac{1}{c}\frac{\partial}{\partial t}\right) u_2^k(L,t), \\ \left(\frac{\partial}{\partial x} - \frac{1}{c}\frac{\partial}{\partial t}\right) u_2^{k+1}(0,t) &= \left(\frac{\partial}{\partial x} - \frac{1}{c}\frac{\partial}{\partial t}\right) u_1^k(0,t), \end{aligned} \tag{5}$$

*lead to well-posed initial boundary value problems even without overlap and they are optimal: convergence in the Schwarz algorithm with these transmission conditions is achieved in two iterations, i.e. $u_i^2$ is identical to $u$ in $\Omega_i$.*

Table 1 shows the convergence to the accuracy of the numerical scheme of the algorithm with transmission conditions (5), without overlap. The velocity is $c = 1$, the computation is done on $(0, T)$ with $T = 2$. The initial data are $u(x, 0) = e^{-50(0.5-x)^2}$, $\partial_t u(x, 0) = 0$. The domain $(0, 2)$ is divided into two subdomains $(0, 1)$ and $(1, 2)$. The initial guess $(u_i^0)_{i=1,2}$ is chosen to be 0. We use the scheme presented in section 3.

| grid | error after 2 iterations | discretization error |
|---|---|---|
| 50 x 50 | 2.6128e-04 | 2.1515e-02 |
| 100 x 100 | 2.7305e-05 | 4.9472e-03 |
| 200 x 200 | 3.2361e-60 | 1.2218e-03 |
| 400 x 400 | 3.9852e-07 | 3.0321e-04 |
| 800 x 800 | 4.9532e-08 | 7.5567e-05 |

Table 1: Convergence in two iterations to the accuracy of the numerical scheme

In view of Theorem 2, we introduce now a general method on non overlapping subdomains.

## 2.1. The general method

We decompose the domain $\mathbb{R}$ into $I$ non overlapping subdomains $\Omega_i = (a_i, a_{i+1})$, $a_j < a_i$ for $j < i$ and $a_1 = -\infty$, $a_{I+1} = \infty$ as given in Figure 2.

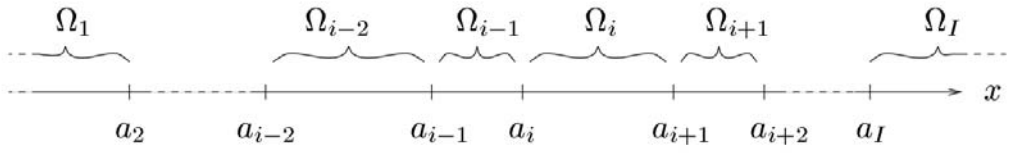


Figure 2: Domain decomposition into $I$ non-overlapping subdomains.

We introduce a general non overlapping Schwarz waveform relaxation algorithm

$$\begin{array}{rcll} \mathcal{L}(u_i^{k+1}) & = & 0 & \text{in } \Omega_i \times (0,T), \\ \mathcal{B}_i^-(u_i^{k+1})(a_i,t) & = & \mathcal{B}_i^-(u_{i-1}^k)(a_i,t) & t \in (0,T), \\ \mathcal{B}_i^+(u_i^{k+1})(a_{i+1},t) & = & \mathcal{B}_i^+(u_{i+1}^k)(a_{i+1},t) & t \in (0,T), \\ u_i^{k+1}(x,0) & = & p(x) & x \in \Omega_i, \\ \frac{\partial u_i^{k+1}}{\partial t}(x,0) & = & q(x) & x \in \Omega_i, \end{array} \tag{6}$$

where $\mathcal{B}_i^{\pm}$ are linear transmission operators which we will determine to get optimal performance of the algorithm. For ease of notation we defined here $u_0^k := 0, \quad u_{I+1}^k := 0$, so that the index $i$ in (6) ranges from $i = 1$ to $I$.

**Definition 1.** The Dirichlet to Neumann operators for the wave equation $\mathcal{S}^-(x_0)$ and $\mathcal{S}^+(x_0)$ are defined as follows. $\mathcal{S}^-(x_0)g(t) = \frac{\partial v}{\partial x}(x_0,t)$, where $v(x,t)$ is the solution of the exterior problem

$$\begin{array}{rcll} \mathcal{L}(v) & = & 0 & \text{in } (-\infty, x_0) \times (0,T), \\ \dfrac{\partial v}{\partial t}(x_0,t) & = & g(t) & t \in (0,T), \end{array} \tag{7}$$

with zero initial data, and $\mathcal{S}^+(x_0)g(t) = \frac{\partial v}{\partial x}(x_0,t)$ where $v(x,t)$ is the solution of the exterior problem

$$\begin{array}{rcll} \mathcal{L}(v) & = & 0 & \text{in } (x_0, \infty) \times (0,T), \\ \dfrac{\partial v}{\partial t}(x_0,t) & = & g(t) & t \in (0,T), \end{array} \tag{8}$$

with zero initial data.

The general result reads

**Theorem 3.** *Algorithm (6) converges in $I$ iterations on $[0,T]$ to the solution $u$ of the wave equation in $\mathbb{R}$ such that $\partial_t u$ and $\partial_x u$ are continuous across the numerical interfaces, for the following choice of the operators $\mathcal{B}_i^{\pm}$:*

$$\mathcal{B}_i^- = (\partial_x - \mathcal{S}^-(a_i)\partial_t), \quad \mathcal{B}_i^+ = (\partial_x + \mathcal{S}^+(a_{i+1})\partial_t).$$

*Proof.* The proof is general and goes as follows. We consider vanishing initial data. At step 1, we have $\mathcal{L}(u_i^1) = 0$ in $\Omega_i = (a_i, a_{i+1})$. Thus by definition we have on the left $\mathcal{B}_2^-(u_1^1)(a_2,\cdot) = 0$. At step 2, the problem in $\Omega_2$ has as a left boundary condition $\mathcal{B}_2^-(u_2^2)(a_2,\cdot) = 0$. We define $\widetilde{\Omega}_2 = (a_1, a_3)$ and $\tilde{u}_2^2$ in $\widetilde{\Omega}_2$ as $u_1^2$ in $\Omega_1$ and $u_2^2$ in $\Omega_2$. We define likewise $\widetilde{\Omega}_{I-1}$ and $\tilde{u}_{I-1}^2$. We now have an equivalent domain decomposition with $(\widetilde{\Omega}_2, \Omega_3, \cdots, \Omega_{I-2}, \widetilde{\Omega}_{I-1})$, and the functions $(\tilde{u}_2^2, u_3^2, \cdots, u_{I-2}^2, \tilde{u}_{I-1}^2)$. We proceed until the problem is reduced to two or three domains, depending on $I$. Suppose $I$ is even. After $K = I/2$ steps we are led to two domains $\widetilde{\Omega}_K = (a_1, a_{K+1})$ and $\widetilde{\Omega}_{K+1} = (a_{K+1}, a_{I+1})$, and two functions $\tilde{u}_K^K$ and $\tilde{u}_{K+1}^K$ such that $\mathcal{L}(\tilde{u}_i^K) = 0$ in $\widetilde{\Omega}_i$. Then due to the exact transmission conditions we have, at step $K+1$, vanishing boundary conditions for $\tilde{u}_K^{K+1}$ and $\tilde{u}_{K+1}^{K+1}$, thus $\tilde{u}_K^{K+1}$ and $\tilde{u}_{K+1}^{K+1}$ vanish. We now have to go successively downwards with vanishing data to $u_{K-1}^{K+1} = 0, \cdots, u_1^{2K} = 0$ and the same upwards. Thus at step $I$, the error vanishes in every subdomain. □

## 2.2. The optimal method in a stratified medium and time windows

Suppose now the velocity to be constant in each subdomain : $c \equiv c_i$ in $\Omega_i$. We then have

**Theorem 4.** *Suppose the subdomains coincide with the discontinuities. Then algorithm (6) converges in two iterations if*

$$\mathcal{B}_i^- = (\partial_x - \frac{1}{c_{i-1}}\partial_t), \quad \mathcal{B}_i^+ = (\partial_x + \frac{1}{c_{i+1}}\partial_t), \tag{9}$$

*and* $T < T_1 = \min_{1<i<I} \dfrac{|a_{i+1} - a_i|}{c_i}$.

This analysis suggests to use time windows on intervals $[pT_1, (p+1)T_1]$ , where $T_1$ is given in theorem 4 and $p$ takes integer values. In each window the algorithm is exact in two iterations.

We now concentrate on the discretization of algorithm (6), with local transmission operators $\mathcal{B}_i^{\pm}$ given by (9). In the case of discontinuous speed, we suppose that $T \leq T_1$, which implies by Theorem 3 that $u_i^2 \equiv u/_{\Omega_i}$ for $1 \leq i \leq I$.

# §3. The numerical algorithm

Each domain $\Omega_i$ is discretized with a mesh $\Delta x_i$, the points are numbered from 0 to $J_i + 1$. The time interval in $\Omega_i$ is discretized with a mesh $\Delta t_i$, and the time steps are numbered from 0 to $N_i + 1$. The discrete value in domain $\Omega_i$, at point $j$ and time $n$ is written $U_i(j,n)$.
In order to handle more easily the boundary conditions, we choose a "vertex centered" finite volume scheme [4]. The displacement u is considered to be constant on the cell $(x - \Delta x/2, x + \Delta x/2) \times (t - \Delta t/2, t + \Delta t/2)$ and the derivatives are constant on the dual mesh.

## 3.1. Description of the scheme

We consider first the boundary value problem defined as the wave equation in each domain $\Omega_i$, with boundary conditions $\mathcal{B}_i^- u_i(a_i) = g_i^-(a_i)$ and $\mathcal{B}_i^+ u_i(a_{i+1}) = g_i^+(a_{i+1})$. We write the interior scheme by integrating the equation on $(x_j - \Delta x_i/2, x_j + \Delta x_i/2) \times (t_n - \Delta t_i/2, t_n + \Delta t_i/2)$, and approximating the remaining derivatives by finite differences. We obtain the classical leapfrog scheme. We now integrate the equation on the half-cell $(a_i, a_i + \Delta x_i/2) \times (t_n - \Delta t_i/2, t_n + \Delta t_i/2)$. We get the same terms as before, but a boundary term which is the integral of $\partial u/\partial x$ on $(t_n - \Delta t_i/2, t_n + \Delta t_i/2)$. It is handled using the boundary condition, and we obtain for example on the left.

$$B_i^-(U_i)(0,n) := \left(\frac{\Delta x_i}{2C_i^2} D_t^+ D_t^- - D_x^+ + \frac{1}{C_{i-1}} D_t^0\right)(U_i)(0,n) = G_i^-(n),$$

where $D_t^+\phi(n) = \frac{1}{\Delta t_i}(\phi(n+1) - \phi(n))$, $D_t^-\phi(n) = \frac{1}{\Delta t_i}(\phi(n) - \phi(n-1))$, $D_t^0\phi(n) = \frac{1}{2\Delta t_i}(\phi(n+1) - \phi(n-1))$ and the same for the $x-$ derivatives. The right hand side is

$$G_i^-(n) := \frac{1}{\Delta t_i} \int_{t_n - \Delta t_i/2}^{t_n + \Delta t_i/2} g_i^-(\tau) d\tau,$$

Within the iterative algorithm, $G_i^-(n)$ is now a $G_i^{-,k}(n)$ , whose value is extracted from $\Omega_{i-1}$ at step $k-1$ using the same process. We define

$$\widetilde{B}_i^-(U_{i-1})(J_{i-1}+1, n) := \left(-\frac{\Delta x_{i-1}}{2C_{i-1}^2} D_t^+ D_t^- - D_x^- + \frac{1}{C_{i-1}} D_t^0\right)(U_{i-1})(J_{i-1}+1, n),$$

and $\widetilde{G}_{i-1}^{-,k-1}(n) = \widetilde{B}_i^-(U_{i-1}^{k-1})(J_{i-1}+1, n)$. If the time steps are the same in $\Omega_i$ and $\Omega_{i-1}$, the transmission condition leads to $G_i^{-,k} = \widetilde{G}_{i-1}^{-,k-1}$. If we have different time grids $\Delta t_i$ in $\Omega_i$. $G_i^{-,k}$ is a vector in $\mathbb{R}^{N_i+1}$ and $\widetilde{G}_i^{-,k-1}$ is a vector in $\mathbb{R}^{N_{i-1}+1}$. We need a projection operator, defined as follows. Suppose we are given a vector $\mathbf{v} = (v_0, \ldots, v_N) \in \mathbb{R}^{N+1}$ which represents the values of a step function on the corresponding intervals $I_n = (t_n, t_{n+1})$ where $t_0 = 0$, $t_{N+1} = T$ and $\cup_{n=0}^N \overline{I_n} = [0,T]$ and the intervals do not overlap. Then we define the scalar product on $\mathbb{R}^{N+1}$ by

$$(\mathbf{v}, \mathbf{w})_{N+1} := \sum_{n=0}^{N} |I_n| v_n w_n,$$

where $|I_n|$ denotes the length of the interval $I_n$. We thus obtain the induced norm on $\mathbb{R}^{N+1}$

$$||\mathbf{v}||_{N+1}^2 := (\mathbf{v}, \mathbf{v})_{N+1}.$$

We first define the operator $\mathbb{F} : \mathbb{R}^{N+1} \longrightarrow L^2(0,T)$ which constructs a piecewise constant function on the intervals $I_n$ from the vector $\mathbf{v}$,

$$\mathbb{F} : \mathbf{v} \longmapsto f(t) := v_n, \quad t \in I_n.$$

Then we define the operator $\mathbb{E} : L^2(0,T) \longrightarrow \mathbb{R}^{N+1}$ which projects a given function $f(t)$ onto a vector $\mathbf{v} \in \mathbb{R}^{N+1}$ corresponding to a piecewise constant function in the intervals $I_n$

$$\mathbb{E} : f(t) \longmapsto v_n := \frac{1}{|I_n|} \int_{I_n} f(t) dt.$$

Denoting by $\mathbb{F}_i$ and $\mathbb{E}_i$ the corresponding operators using the grid of $\Omega_i$, we define the operator $\mathbb{P}_{i,j} : \mathbb{R}^{N_i+1} \longrightarrow \mathbb{R}^{N_j+1}$ by

$$\mathbb{P}_{i,j} := \mathbb{E}_j \circ \mathbb{F}_i. \tag{10}$$

The precise implementation of the projection procedure is described in [6]. With these notations we have on the left $G_i^{-,k} = \mathbb{P}_{i,i-1}\widetilde{G}_{i-1}^{-,k-1}$, and the same on the right.
We obtain the discrete Schwarz waveform relaxation algorithm on subdomains $\Omega_i$, $1 \leq i \leq I$ with non-matching grids:

**Definition 2.** The discrete algorithm corresponding to (6,9) is given by

$$\left(\frac{1}{C_i^2(j)}D_t^+D_t^- - D_x^+D_x^-\right)(U_i^{k+1})(j,n) = 0, \quad 1 \leq j \leq J_i,\ 1 \leq n \leq N_i, \tag{11}$$

$$B_i^-(U_i^{k+1})(0,\cdot) = \mathbb{P}_{i-1,i}\widetilde{B}_i^-(U_{i-1}^k)(J_{i-1}+1,\cdot), \tag{12}$$

$$B_i^+(U_i^{k+1})(J_i+1,\cdot) = \mathbb{P}_{i+1,i}\widetilde{B}_i^+(U_{i+1}^k)(0,\cdot), \tag{13}$$

with the discrete operators

$$\begin{aligned} B_i^-(U_i)(0,n) &= \left(\tfrac{\Delta x_i}{2C_i^2}D_t^+D_t^- - D_x^+ + \tfrac{1}{C_{i-1}}D_t^0\right)(U_i)(0,n), \\ \widetilde{B}_i^-(U_{i-1})(J_{i-1}+1,n) &= \left(-\tfrac{\Delta x_{i-1}}{2C_{i-1}^2}D_t^+D_t^- - D_x^- + \tfrac{1}{C_{i-1}}D_t^0\right)(U_{i-1})(J_{i-1}+1,n), \end{aligned} \tag{14}$$

$$\begin{aligned} B_i^+(U_i)(J_i+1,n) &= \left(\tfrac{\Delta x_i}{2C_i^2}D_t^+D_t^- + D_x^- + \tfrac{1}{C_{i+1}}D_t^0\right)(U_i)(J_i+1,n), \\ \widetilde{B}_i^+(U_{i+1})(0,n) &= \left(-\tfrac{\Delta x_{i+1}}{2C_{i+1}^2}D_t^+D_t^- + D_x^+ + \tfrac{1}{C_{i+1}}D_t^0\right)(U_{i+1})(0,n), \end{aligned} \tag{15}$$

provided with initial values derived in the same way.

We note on formulae (14,15) that the transport operators $\mathcal{B}_i^{\pm}$ are approximated by a Lax-Wendroff scheme, and that they are discretized differently depending on whether they apply to $U_i$ or to $U_{i\pm1}$.

## 3.2. The case of continuous wave speed across numerical interfaces

We denote by $V = \{V(j)\}_{0\leq j\leq J+1}$ a sequence in $\mathbb{R}^{J+2}$, and we define for $V, W \in \mathbb{R}^{J+2}$ a bilinear form on $\mathbb{R}^{J+2}$ by

$$a_h(V,W) = \frac{\Delta x}{2}\sum_{j=1}^{J+1} D_x^-(V)(j)\cdot D_x^-(W)(j). \tag{16}$$

Accordingly, for any positive $n$, $V(n)$ stands for the sequence $\{V(j,n)\}_{0\leq j\leq J+1}$. The discrete energy $E_n$ at time step $n$, global in space, is defined as the sum of a discrete kinetic energy $E_{K,n}$ and a discrete potential energy $E_{P,n}$ given by

$$\begin{aligned} E_{K,n} &= \frac{\Delta x}{2}\left[\frac{1}{2C^2(0)}(D_t^-(V)(0,n))^2 + \sum_{j=1}^{J}\frac{1}{C^2(j)}(D_t^-(V)(j,n))^2 + \frac{1}{2C^2(J+1)}(D_t^-(V)(J+1,n))^2\right], \\ E_{P,n} &= a_h(V(n), V(n-1)), \\ E_n &= E_{K,n} + E_{P,n}. \end{aligned} \tag{17}$$

The quantity $E_{K,n}$ is clearly a discrete kinetic energy. $E_n$ can be identified as an energy by the

**Lemma 5.** *For any $n \geq 1$, we have*

$$E_n \geq \left(1 - \left(C\frac{\Delta t}{\Delta x}\right)^2\right) E_{K,n}, \tag{18}$$

*where $C$ is defined by $C = \sup_{1\leq j\leq J+1} C(j)$. Hence, under the CFL condition*

$$C\frac{\Delta t}{\Delta x} < 1, \tag{19}$$

*$E_n$ is bounded from below by an energy.*

This provides in each subdomain an energy identity and we proved in [6] the following result.

**Theorem 6.** *Assume that the velocity is continuous on the interfaces $a_i$. If the CFL condition (19) is satisfied by the discretization in each subdomain, then the non-overlapping discrete Schwarz waveform relaxation algorithm (11,...,15) is well-posed and converges on any time interval $[0, T]$ to the solution of*

$$\begin{aligned} \left(\tfrac{1}{C_i^2(j)} D_t^+ D_t^- - D_x^+ D_x^-\right)(U_i)(j,n) &= 0, \quad 1 \leq j \leq J_i,\ 1 \leq n \leq N_i, \\ B_i^-(U_i)(0,\cdot) &= \mathbb{P}_{i-1,i}\widetilde{B}_i^-(U_{i-1})(J_{i-1}+1,\cdot), \\ B_i^+(U_i)(J_i+1,\cdot) &= \mathbb{P}_{i+1,i}\widetilde{B}_i^+(U_{i+1})(0,\cdot), \end{aligned} \tag{20}$$

*in the energy norm, i.e.*

$$\sum_{i=1}^{I} E_{N_i}(U_i^k - U_i) \to 0 \text{ as } k \to \infty.$$

The same calculations actually give a stability result for the limit

**Theorem 7.** *With the same assumptions as in Theorem 6, the limit of the iterates given by (20) satisfies the energy bounds, with a constant $C$ depending only on the $L^2$ norms of the initial conditions:*

$$\sum_{i=1}^{I} E_{N_i}(U_i) \leq C.$$

## 3.3. The case of a stratified medium

We suppose again the velocity to be constant in each subdomain : $c \equiv c_i$ in $\Omega_i$. We define a local CFL number to be $\gamma_i = c_i \Delta t_i / \Delta x_i$. The stability for the pure Cauchy problem implies $\gamma_i \leq 1$ (see for instance[7]).

### *3.3.1. The case $\gamma = 1$*

We suppose here that $\gamma_i = 1$ in every $\Omega_i$. The scheme resumes to

$$U_i(j, n+1) + U_i(j, n-1) - (U_i(j+1, n) + U_i(j-1, n)) = 0, \tag{21}$$

and the discrete operators are given for any solution of (21) by

$$\begin{aligned}\widetilde{B}_2^-(U_1)(J_1+1,n) &= \frac{1}{\Delta x_1}(U_1(J_1,n) - U_1(J_1+1,n-1)),\\ \widetilde{B}_1^+(U_2)(0,n) &= \frac{1}{\Delta x_2}(U_2(1,n) - U_2(0,n-1)).\end{aligned} \tag{22}$$

We consider first two media $\Omega_1 = (-\infty, 0)$ and $\Omega_2 = (0, +\infty)$.

**Theorem 8.** *In the case of two media $\Omega_1$ and $\Omega_2$ with the same CFL number $\gamma_1 = \gamma_2 = 1$, the discrete algorithm (11,12,13) converges in two iterations to the solution of (20).*

*Proof.* It is mimicked on the continuous case. By (21, 22), we have

$$\begin{aligned}\widetilde{B}_2^-(U_1)(J_1+1,n) &= U_1(J_1-n+1,1) - U_1(J_1-n,0),\\ \widetilde{B}_1^+(U_2)(0,n) &= U_2(n,1) - U_2(n-1,0).\end{aligned}$$

Let now the initial values be null. It implies that we have at step 1 $\widetilde{B}_2^-(U_1^1)(J_1+1,\cdot) \equiv 0$ and $\widetilde{B}_2^+(U_2^1)(0,\cdot) \equiv 0$. By linearity we have $B_2^-(U_2^2)(0,\cdot) \equiv 0$ and $B_1^+(U_1^2)(J_1+1,\cdot) \equiv 0$. We conclude that $U_i^2 \equiv U_i$ for $i = 1, 2$. □

When $\gamma$ is equal to 1, the discrete velocity is equal to the continuous speed. Then Theorem 8 extends easily to

**Theorem 9.** *In the case of I media $\Omega_i$ with the same CFL number $\gamma_i = 1$, the discrete algorithm (11,12,13) converges in two iterations to the solution of (20) for $T < T_1$.*

*3.3.2. The case $\gamma < 1$*

We consider two media $\Omega_1 = (-\infty, 0)$ and $\Omega_2 = (0, +\infty)$, with velocities $c_1$ and $c_2 = qc_1$. The space mesh is constant, $\Delta x_1 = \Delta x_2 = \Delta x$, and $\Delta t_1 = q\Delta t_2$. Therefore $\gamma_1 = \gamma_2 = \gamma$.
We analyze here the case $q = 2$. First note that the existence of a solution to (20) is reduced to the question of uniqueness. Let now $U_i$ be the discrete solution of (20) or (11,12,13) with vanishing data. We split $U_2$ in $\Omega_2$ into an even part $\{U_{2P}(\cdot,n)\}_{n\in\mathbb{N}} = \{U_2(\cdot,2n)\}_{n\in\mathbb{N}}$ and an odd part $\{U_{2I}(\cdot,n)\} = \{U2(\cdot,2n+1)\}_{n\in\mathbb{N}}$. We define

$$\begin{aligned}V_1^k = B_1^+(U_1^k)(J_1+1,\cdot) \quad ; \quad V_2^k = B_2^-(U_2^k)(0,\cdot),\\ \widetilde{V}_1^k = \widetilde{B}_2^-(U_1^k)(J_1+1,\cdot) \quad ; \quad \widetilde{V}_2^k = \widetilde{B}_1^+(U_2^k)(0,\cdot).\end{aligned}$$

Hence the projection operators $\mathbb{P}_{i,j}$ have the very special form

$$(\mathbb{P}_{12}V_1)_{2P} = V_1\,; \quad (\mathbb{P}_{12}V_1)_{2I} = V_1\,; \quad \mathbb{P}_{21}V_2 = \frac{1}{2}(V_{2P} + V_{2I}),$$

which gives the transmission conditions as

$$V_{2P}^{k+1} = \widetilde{V}_1^k = V_{2I}^{k+1}; \quad V_1^{k+1} = \frac{1}{2}(\widetilde{V}_{2P}^k + \widetilde{V}_{2I}^k). \tag{23}$$

The discrete Laplace transform of a grid function $v = \{v_n\}_{n\geq 0}$ on a regular grid with time step $\delta t$ is defined for $\eta > 0$ by (see for instance [7])

$$\mathcal{L}v(s) = \hat{v}(s) = \delta t \sum_{n\geq 0} e^{-sn\delta t} v_n, \quad s = \eta + i\tau,\ |\tau| \leq \frac{\pi}{\delta t}. \tag{24}$$

Using the Laplace transform of $U_1, U_{2P}$ and $U_{2I}$ on the mesh $\delta t = 2\Delta t$, equation (11) in $\Omega_1$ becomes the difference equation

$$(e^{2s\Delta t} + e^{-2s\Delta t} - 2)\hat{U}_1 - \gamma_1^2 A\hat{U}_1 = 0, \tag{25}$$

with operator $A$ acting on the $j-$ variables given by

$$Ag(j) = g(j+1) - 2g(j) + g(j-1).$$

Equation (11) in $\Omega_2$ becomes

$$\begin{aligned} &(1 + e^{-2s\Delta t})\,\hat{U}_{2I}(j,s) - 2\hat{U}_{2P}(j,s) - \gamma_2^2 A\hat{U}_{2P} = 0, \\ &(1 + e^{2s\Delta t})\,\hat{U}_{2P}(j,s) - 2\hat{U}_{2I}(j,s) - \gamma_2^2 A\hat{U}_{2I} = 0. \end{aligned} \tag{26}$$

According to the results in [6], we denote by $r_+(z,\gamma)$ (resp.$r_-$ ) the root whose modulus is $> 1$ (resp.$< 1$) for strictly positive $\eta$ of the characteristic equation

$$\gamma^2(r - 2 + 1/r) = (z + 1/z - 2). \tag{27}$$

We then can solve (25) and (26) with $Z = e^{s\Delta t}$ as (see [1] and [3])

$$\begin{aligned} \widehat{U}_1^k(j,s) \qquad &= a_1^k(s)(r_+(Z^2,\gamma_1))^j, \\ \begin{pmatrix} \widehat{U}_{2I}(j,s) \\ \widehat{U}_{2P}(j,s) \end{pmatrix} \quad &= a_{2p}^k(s)(r_-(Z,\gamma_2))^j \begin{pmatrix} Z \\ 1 \end{pmatrix} + a_{2m}^k(s)(r_-(-Z,\gamma_2))^j \begin{pmatrix} -Z \\ 1 \end{pmatrix}. \end{aligned} \tag{28}$$

The boundary terms $\widehat{V}_j^k$ and $\widehat{\widetilde{V}}_j^k$ are given by

$$\begin{aligned} \Delta x_1 \widehat{V}_1^k &= E(Z^2, \gamma, \frac{c_1}{c_2})\, a_1^k, \\ \Delta x_1 \widehat{\widetilde{V}}_1^k &= \widetilde{E}(Z^2, \gamma, 1)\, a_1^k, \end{aligned} \tag{29}$$

$$\begin{aligned} \Delta x_2 \begin{pmatrix} \widehat{V}_{2I}^k(j,s) \\ \widehat{V}_{2P}^k(j,s) \end{pmatrix} &= a_{2p}^k\, E(Z,\gamma,\frac{c_2}{c_1}) \begin{pmatrix} Z \\ 1 \end{pmatrix} + a_{2m}^k\, E(-Z,\gamma,\frac{c_2}{c_1}) \begin{pmatrix} -Z \\ 1 \end{pmatrix} \\ \Delta x_2 \begin{pmatrix} \widehat{\widetilde{V}}_{2I}^k(j,s) \\ \widehat{\widetilde{V}}_{2P}^k(j,s) \end{pmatrix} &= a_{2p}^k\, \widetilde{E}(Z,\gamma,1) \begin{pmatrix} Z \\ 1 \end{pmatrix} + a_{2m}^k\, \widetilde{E}(-Z,\gamma,1) \begin{pmatrix} -Z \\ 1 \end{pmatrix} \end{aligned} \tag{30}$$

with factors $E$ and $\widetilde{E}$ given by

$$\begin{aligned} k(z) = \frac{1}{2}\left(z - \frac{1}{z}\right), \quad \sigma(z,\gamma) = \frac{1}{2}(r_+(z) - r_-(z)), \\ E(z,\gamma,q) = \sigma(z,\gamma) + \frac{q}{\gamma}k(z), \quad \widetilde{E}(z,\gamma,q) = -\sigma(z,\gamma) + \frac{q}{\gamma}k(z). \end{aligned} \tag{31}$$

Transmission conditions (23) become

$$\widehat{V}_{2P}^{k+1} = \widehat{V}_{2I}^{k+1} = \widehat{\widehat{V}}_1^k; \quad \widehat{V}_1^{k+1} = \frac{1}{2}(\widehat{\widehat{V}}_{2P}^k + \widehat{\widehat{V}}_{2I}^k),$$

and thus we get the recursion relations

$$\left| \begin{array}{l} a_{2m}^k = \dfrac{Z-1}{Z+1} \dfrac{E(-Z,\gamma,\frac{c_2}{c_1})}{E(Z,\gamma,\frac{c_2}{c_1})}\, a_{2p}^k, \\ a_{2p}^{k+1} = \dfrac{1}{4} \dfrac{Z+1}{Z} \dfrac{\widetilde{E}(Z^2,\gamma,1)}{E(Z,\gamma,\frac{c_2}{c_1})}\, a_1^k, \\ a_1^{k+1} = \dfrac{1}{Z+1} \dfrac{E(Z,\gamma,\frac{c_2}{c_1})}{E(Z^2,\gamma,\frac{c_1}{c_2})} \left[ (Z+1)^2 \dfrac{\widetilde{E}(Z,\gamma,1)}{E(Z,\gamma,\frac{c_2}{c_1})} - (Z-1)^2 \dfrac{\widetilde{E}(-Z,\gamma,1)}{E(-Z,\gamma,\frac{c_2}{c_1})} \right] a_{2p}^k. \end{array} \right. \tag{32}$$

There is a two-level recursion formula for each coefficient $a_j^{k+2} = R a_j^k$, with a convergence rate

$$R(Z,\gamma) = \frac{1}{4Z} \frac{\widetilde{E}(Z^2,\gamma,1)}{E(Z^2,\gamma,\frac{c_1}{c_2})} \left[ (Z+1)^2 \frac{\widetilde{E}(Z,\gamma,1)}{E(Z,\gamma,\frac{c_2}{c_1})} - (Z-1)^2 \frac{\widetilde{E}(-Z,\gamma,1)}{E(-Z,\gamma_2,\frac{c_2}{c_1})} \right]. \tag{33}$$

Defining

$$\rho(z,\gamma,q) = \frac{\widetilde{E}(z,\gamma,1)}{E(z,\gamma,q)}; \quad \tilde{\rho}(Z,\gamma) = \frac{(Z+1)^2}{4Z} \rho(Z,\gamma,\frac{c_1}{c_2})\, \rho(Z^2,\gamma,\frac{c_2}{c_1}), \tag{34}$$

we obtain for the convergence rate of the discrete Schwarz waveform relaxation algorithm

$$R(Z,\gamma) = \tilde{\rho}(Z,\gamma) - \tilde{\rho}(-Z,\gamma). \tag{35}$$

The properties of the solutions $r^{\pm}(z)$ and of the functions $E$ and $\widetilde{E}$ are given in great details in [6]. In particular it is proved that for any $z \neq 1$, and $\gamma < 1$, $E(z,\gamma,q) \neq 0$. Furthermore if $z \to 1$, we have

$$E(z,\gamma,q) = \mathcal{O}(z-1); \quad \widetilde{E}(z,\gamma,1) = \mathcal{O}((z-1)^3).$$

Thus $\tilde{\rho}$ is well-defined for $|z| > 1$, with $\tilde{\rho}(1,\gamma) = 0$, and so is $R$. The convergence rate $R(z,\gamma)$ is an analytic function of $z$ for $|z| \geq 1$, which corresponds to $\eta \geq 0$. $R$ satisfies a maximum principle for $\eta \geq 0$ and hence attains its maximum on the boundary $\eta = 0$. It is therefore sufficient to study the behavior of $R$ for $\eta = 0$.

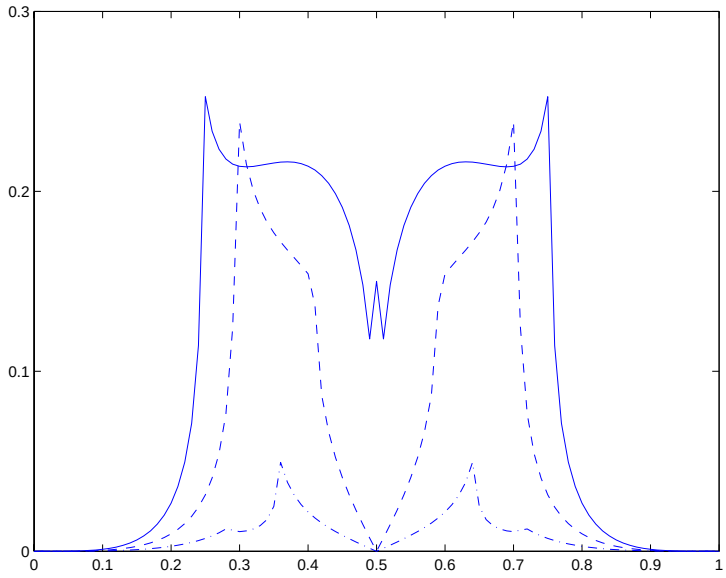


Figure 3: variation of $|R(e^{i\tau\Delta t},\gamma)|$ as a function of $\tau\Delta t$ for various values of $\gamma$.$\gamma = 0.7$, solid, $\gamma = 0.8$, dash, $\gamma = 0.9$, dash-dot.

**Lemma 10.** *There exists a strictly positive constant $K$ such that the convergence rate satisfies*

$$\sup_{|z|=1} |R(z,\gamma,c_1/c_2)| \leq K < 1.$$

and we conclude as in [6]:

**Theorem 11.** *The scheme (20) is well-posed in the GKS sense. Furthermore let $U_i^p$ be the iterates of algorithm (11,12,13) with the same initial values. Then we have*

$$\|U_i^p - U_i\|_{\Omega_i\times(0,T)} \leq (K)^{\lfloor \frac{p}{2} \rfloor} max_{i=1,2} \left\|U_i^0 - U_i\right\|_{\Omega_i}.$$

*where* $\|U_i\|^2_{\Omega_i\times(0,T)} = \Delta t_i \Delta x_i \sum_n \sum_j |U_i(j,n)|^2$ *and* $\|U_i^0\|^2_{\Omega_i} = \Delta x_i \sum_j |U_i^0(j)|^2$.

## §4. Numerical results

We first compare our method to two other refinement methods. They do not involve domain decomposition, and have been analyzed in the case when the velocity is equal to 1 and one domain is a refinement of the neighbour.

### 4.1. Some comparisons in the case of two half-spaces

We restrict ourselves to the case where $c = 1$ and $(\Delta t_1, \Delta x_1) = (2\Delta t_2, 2\Delta x_2) = (2\Delta t, 2\Delta x)$. The first method, we call the I-method, consists in defining three transmission conditions as follows. $U_1(0,n)$ is obtained by the leapfrog scheme on the dotted stencil in Figure 4. Then continuity is enforced on the even points : $U_2(0,2n) = U_1(0,n)$, and interpolation at odd points: $U_2(0,2n+1) = \frac{1}{2}(U_1(0,n) + U_1(0,n+1))$. A complete analysis of stability for the

Lax-Wendroff scheme can be found in [1].

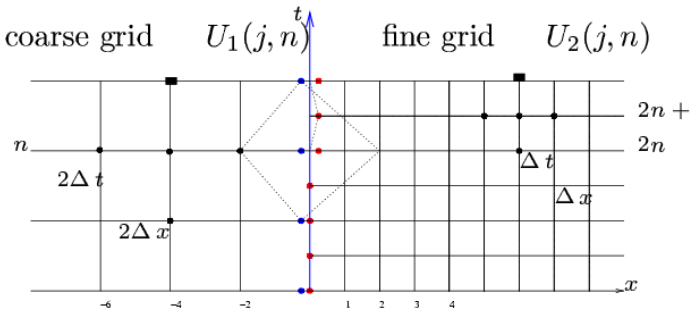


Figure 4: the I-method

In the second method, we call E-method developed in [2], three relations are written between $U_1$ and $U_2$ which preserve the energy in both domains. They are too complicated to be written here.
The test case is the same as in [3]. $\Omega_1 = (0, 100)$ with transparent boundary condition on the left, and $\Omega_2 = (100, 110)$ with a transparent boundary condition on the right. The initial condition is drawn in Figure 5.

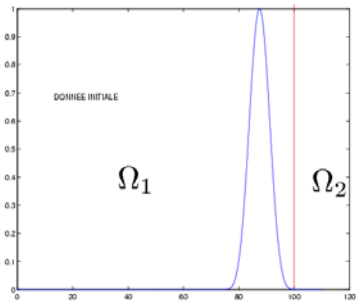


Figure 5: Initial value

The time $T$ is equal to 200. The space mesh is fixed equal to $\Delta x = 0.5$, and we take various values of $\Delta t$.
We start with the case $\gamma_1 = \gamma_2 = 1$ in Table 2. In this case a uniform mesh would produce an exact scheme as mentioned in the first paragraph. As noted by the authors in [2], the E-method produces wrong results. In the coarse domain, the scheme is exact. In the right domain, interpolation is better by a factor of 2.

| | max error in $\Omega_1$ | max error in $\Omega_2$ |
|---|---|---|
| scheme error, fine grid | 1.6098e-15 | 1.4988e-15 |
| D.D-method | 1.8319e-15 | 0.0089 |
| I-method | 1.9429e-15 | 0.0046 |
| E-method | 1.9971e-04 | 0.4949 |

Table 2: error in $L^\infty(\Omega_i \times (0,T))$ for $\gamma_1 = \gamma_2 = 1$

We now reduce the coefficient $\gamma$, to $\gamma = 0.9091$ in table 3. The three methods are comparable on the left domain, in the right domain the interpolation method is the best, there is a factor 2 with the DD-method, and a factor 16 with the E-method.

| | max error in $\Omega_1$ | max error in $\Omega_2$ |
|---|---|---|
| scheme error, fine grid | 0.0022 | 0.0006 |
| scheme error, coarse grid | 0.009 | 0.003 |
| D.D-method | 0.0068 | 0.0064 |
| I-method | 0.0068 | 0.0027 |
| E-method | 0.0068 | 0.0437 |

Table 3: error in $L^\infty(\Omega_i \times (0,T))$ for for $\gamma_1 = \gamma_2 = 0.9091$

We will not diminish $\gamma$ further, since then the dispersion error would be too large.
In [2] is shown an example with a Dirichlet boundary condition on the right. In that case the I-method is unstable. We reproduce their example in Figure 6. The velocity is constant equal to 1. The domains are $\Omega_1 = (0, 100)$, $\Omega_2 = (100, 103.5)$, $T = 1000$. The space meshes are the same in both domains equal to 1,$\gamma_1 = \gamma_2 = 0.913$.

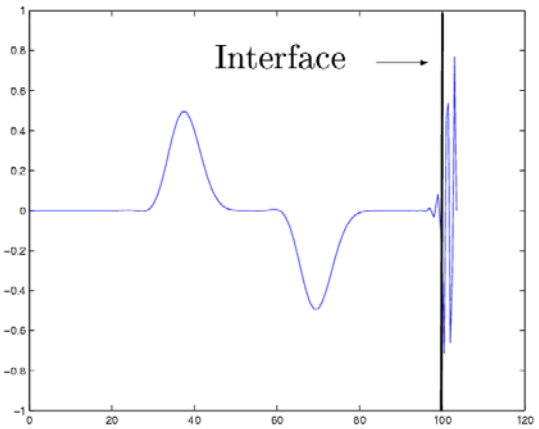


Figure 6: Solution of the I-method in $\Omega_1 \cup \Omega_2$ for Dirichlet boundary condition after 400 timesteps

This phenomenon is also reported in [1] as a personal communication of Oliger. No detailed proof is avalaible so far. Another case is where we modify $\Omega_2$ and $\gamma$ a little, taking $\Omega_2 =$

$(100, 110)$, $\gamma = 0.9524$. The numerical data are the same as before. The scheme remains stable, and we have the errors inTtable 4.

| | max error in $\Omega_1$ | max error in $\Omega_2$ |
|---|---|---|
| scheme error, fine grid | 0.0265 | 0.0265 |
| scheme error, coarse grid | 0.1050 | 0.1050 |
| D.D-method | 0.0764 | 0.0693 |
| I-method | 0.0471 | 0.0425 |
| E-method | 0.0781 | 0.1062 |

Table 4: error in $L^\infty(\Omega_i \times (0, T))$ for Dirichlet boundary condition, $\gamma_1 = \gamma_2 = 0.9524$

Here the I-method is the best, followed by the present method, especially in the fine grid. In Figure 7 we draw the $L^\infty$ error in time and space in both domains as a function of the mesh, for the same data. We see that the present method is of order 2.

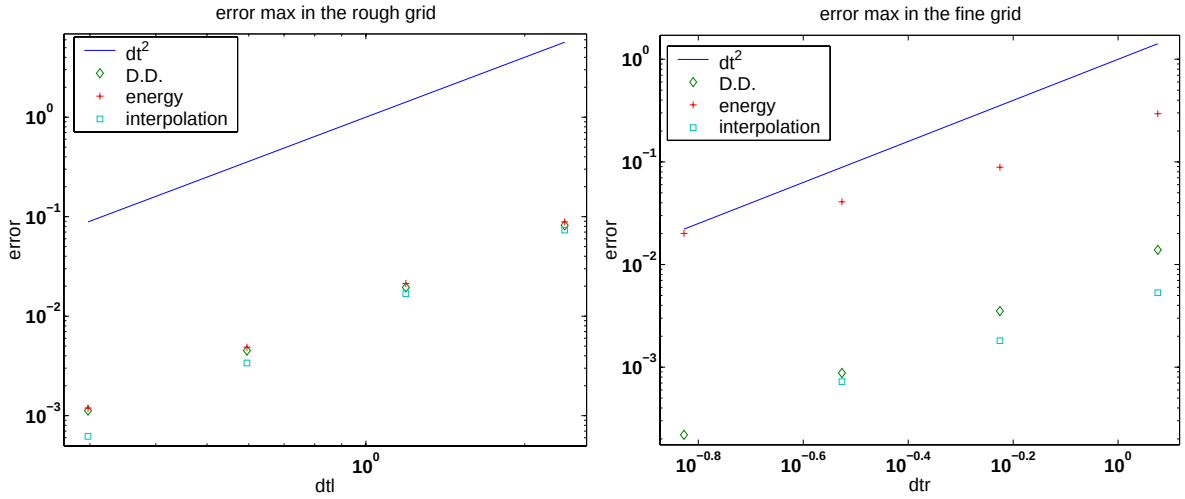


Figure 7: error in $L^\infty(\Omega_i \times (0, T))$ as a function of the time step, logarithmic scale. On the left the coarse grid, on the right the fine grid. Comparison between the three methods

## 4.2. A few more difficult cases

The domains are $\Omega_1 = (0, 1), \Omega_2 = (1, 2)$, $T = 1$. The velocity are c=1 in $\Omega_1$, c=1.7 in $\Omega_2$. The initial data is as in Figure 5, supported in $\Omega_1$. We choose first 11 points in space in each domain, and the number of points in time such that $\gamma = 1$ in both domains, that is 11 points in time in $\Omega_1$ and 18 in $\Omega_2$. Thereafter the meshes are divided by 2. In Figure 8 we draw the $L^\infty$ error in time and space in both domains as a function of the mesh, and we see that the method is still of order 2.

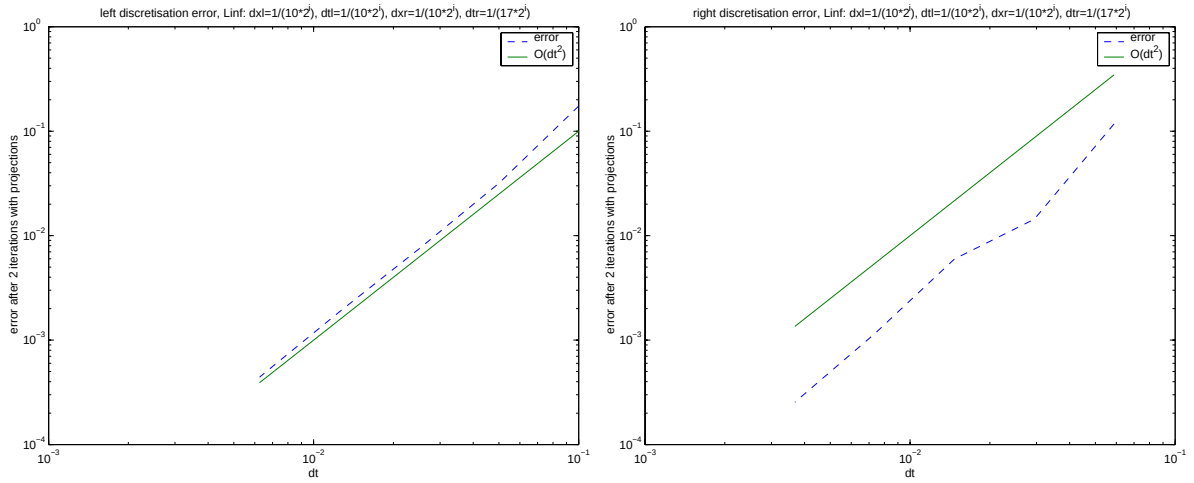


Figure 8: error in $L^\infty(\Omega_i \times (0,T))$ as a function of the time step, logarithmic scale. On the left the coarse grid, on the right the fine grid.

We consider now the space interval $[0,6]$ divided in 6 layers $c_i \in \{1, 2/3, 1/2, 3/4, 4/5\}$. The six numerical domains are aligned with the discontinuities. We chose the same space mesh in the subdomains, $\Delta x_i = 1/50$, and the local time steps are such that $\gamma_i$ is close to 1. The time interval is $[0,1]$.

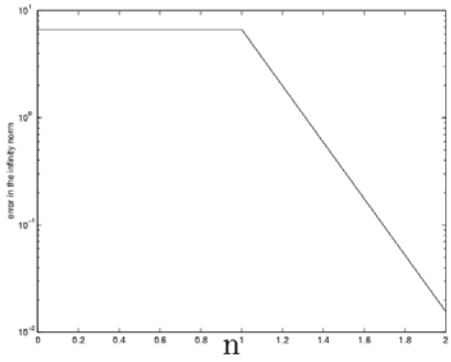


Figure 9: Convergence in 2 iterations with local transmission conditions on time interval [0 1]

## §5. Conclusions

We have proposed a new way of considering the mesh refinement problem. Applied to the leapfrog scheme, we have proven it to be stable, and given numerical evidence of an order 2 in time. The precise study of the accuracy will be done in a forthcoming paper. Its flexibility allows for the use of other schemes, like finite elements in time and space for instance, and other equations. It is robust and will extend to higher dimensions.

## Acknowledgements

The author is grateful to M.J. Gander for providing the original scripts of the numerical method described first in [6].

## References

[1] BERGER, M. Stability of interfaces with mesh refinement. *Math. of Comp. 45*, 172 (1985), 301–318.

[2] COLLINO, F., FOUQUET, T. AND JOLY, P A conservative space-time mesh refinement method for the 1D Wave equation. Part I : construction. *Numer. Math. 95*, (2003), 197–221.

[3] COLLINO, F., FOUQUET, T. AND JOLY, P A conservative space-time mesh refinement method for the 1D Wave equation. Part II : analysis. *Numer. Math. 95*, (2003), 223–251.

[4] GALLOUËT, T.,HERBIN, R. AND VIGNAL, M.H. Error estimates for the approximate finite volume solution of convection diffusion equations with general boundary conditions. *SIAM J. Numer. Anal. 37*, 6(2000), 1935–1972.

[5] GANDER, M. Analysis of parallel algorithms for time dependent partial differential equations. *Phd Thesis, Stanford, CA 94305, USA*, 1997.

[6] GANDER, M., HALPERN, L. AND NATAF, F. Optimal Schwarz waveform relaxation for the one-dimensional wave equation. *SIAM J. Numer. Anal.* ,6(2004), 1935–1972.

[7] STRIKWERDA, J.C. *finite difference schemes and partial differential equations*. Chapman and Hall,1989.

Laurence Halpern
LAGA. Institut Galilée
Université Paris 13.
93430 Villetaneuse. France.
halpern@math.univ-paris13.fr